

Determination of the thermal conductivity tensor of the $n=7$ Aurivillius phase $\text{Sr}_4\text{Bi}_4\text{Ti}_7\text{O}_{24}$

M. A. Zurbuchen, D. G. Cahill, J. Schubert, Y. Jia, and D. G. Schlom

Citation: *Appl. Phys. Lett.* **101**, 021904 (2012); doi: 10.1063/1.4733616

View online: <http://dx.doi.org/10.1063/1.4733616>

View Table of Contents: <http://apl.aip.org/resource/1/APPLAB/v101/i2>

Published by the [American Institute of Physics](http://www.aip.org).

Additional information on *Appl. Phys. Lett.*

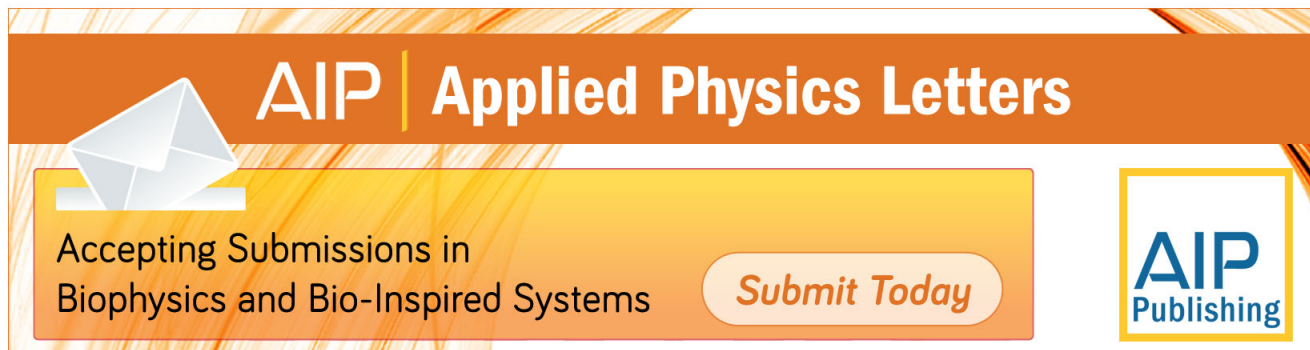
Journal Homepage: <http://apl.aip.org/>

Journal Information: http://apl.aip.org/about/about_the_journal

Top downloads: http://apl.aip.org/features/most_downloaded

Information for Authors: <http://apl.aip.org/authors>

ADVERTISEMENT

An advertisement banner for Applied Physics Letters. It features a dark orange background with a lighter orange gradient at the bottom. On the left, there is a white envelope icon. The text 'AIP | Applied Physics Letters' is prominently displayed in white. Below this, the text 'Accepting Submissions in Biophysics and Bio-Inspired Systems' is written in black. To the right of this text is a white button with the text 'Submit Today' in orange. In the bottom right corner, there is a logo for 'AIP Publishing' in blue and white.

AIP | Applied Physics Letters

Accepting Submissions in
Biophysics and Bio-Inspired Systems

Submit Today

AIP
Publishing

Determination of the thermal conductivity tensor of the $n = 7$ Aurivillius phase $\text{Sr}_4\text{Bi}_4\text{Ti}_7\text{O}_{24}$

M. A. Zurbuchen,^{1,a)} D. G. Cahill,² J. Schubert,³ Y. Jia,⁴ and D. G. Schlom^{4,5}

¹Department of Materials Science and Engineering, University of California, Los Angeles, California 90095, USA

²Department of Materials Science and Engineering, Materials Research Laboratory, University of Illinois, Urbana, Illinois 61801, USA

³Institut für Schichten und Grenzflächen and Center of Nanoelectronic Systems for Information Technology, Forschungszentrum Jülich GmbH, D-52425 Jülich, Germany

⁴Department of Materials Science and Engineering, Cornell University, Ithaca, New York 14853, USA

⁵Kavli Institute at Cornell for Nanoscale Science, Ithaca, New York 14853, USA

(Received 16 May 2012; accepted 18 June 2012; published online 11 July 2012)

A challenge in the preparation of advanced materials that exist only as thin films is to establish their properties, particularly when the materials are of low symmetry or the tensor properties of interest are of high rank. Using $\text{Sr}_4\text{Bi}_4\text{Ti}_7\text{O}_{24}$ as an example, we show how the preparation of oriented epitaxial films of multiple orientations enables the thermal conductivity tensor of this tetragonal material with a c -axis length of 64.7 Å to be measured. The thermal conductivity tensor coefficients $k_{33} = 1.10 \text{ W m}^{-1} \text{ K}^{-1}$ and $k_{11} = k_{22} = 1.80 \text{ W m}^{-1} \text{ K}^{-1}$ were determined by growing epitaxial $\text{Sr}_4\text{Bi}_4\text{Ti}_7\text{O}_{24}$ films on (100), (110), and (111) SrTiO_3 substrates. © 2012 American Institute of Physics. [<http://dx.doi.org/10.1063/1.4733616>]

Nanoscale thermal transport is an area of intense interest,¹ and ultra-low thermal conductivities are of specific interest for thermal barrier coatings or potential thermal isolation layers in microelectronics. Recent work in nano-scale oxide superlattices has revealed some surprising properties, such as those of $\text{CsBiNb}_2\text{O}_7$, with a thermal conductivity significantly below the amorphous limit at room temperature.^{2,3} The anisotropy of thermal transport in these materials is an area that is just beginning to be explored in bulk and in thin films.^{4,5} Also of interest are trends in thermal conductivity with changes in dimensionality from two-dimensional to three-dimensional materials (i.e., with increasing superlattice period where the superlattice interfaces are phonon scatterers).⁶

Natural superlattice phases, which can be synthesized in bulk form, are the most straightforward to probe. Some "engineered" superlattice phases can only be synthesized through highly controlled deposition processes, for example, the layered oxides $\text{Sr}_{n+1}\text{Ti}_n\text{O}_{3n+1}$,⁷⁻¹⁰ $\text{Sr}_{n+1}\text{Ru}_n\text{O}_{3n+1}$,¹¹ and $\text{Bi}_7(\text{Mn,Ti})_6\text{O}_{21}$ (Refs. 12 and 13) which have been made using pulsed-laser deposition (PLD) or oxide molecular-beam epitaxy (MBE). This is because bulk synthesis of long-period natural superlattice phases is limited by thermodynamic degeneracy.^{14,15} The free energy difference between successive members of a homologous series becomes diminishingly small, and phase coexistence tangents merge into a curve, resulting in a lack of thermodynamic driving force to stabilize an individual member of a homologous series of phases.

The layered perovskite phase $\text{Sr}_4\text{Bi}_4\text{Ti}_7\text{O}_{24}$, a member of the Aurivillius family of phases, $\text{Bi}_2\text{A}_{n-1}\text{B}_n\text{O}_{3n+3}$,¹⁶ is beyond the outskirts of being a thermodynamically stable bulk phase, and has previously been synthesized only via epitaxial stabilization in thin film form.¹³ Its structure is shown schematically in Fig. 1, along with other members of

the series. These bismuth-layered oxides consist of $\text{Bi}_2\text{O}_2^{2+}$ layers alternating with n number of ABO_3 perovskite units. Epitaxial growth on various cuts of perovskite substrates can be used to control the orientation of lower- n Aurivillius phases, creating essentially single-crystal-like material. Such films do form rotational twin (or growth twin) domains, which arise from the energetically degenerate ways in which these phases can epitaxially orient to the substrate surface.¹⁷⁻²¹ The two-fold surface of (110) SrTiO_3 yields two rotational twins, and the three-fold surface of (111) SrTiO_3 yields three rotational twins, as shown schematically in Fig. 2. This is similar to the previously demonstrated epitaxial relationship for $\text{SrBi}_2\text{Nb}_2\text{O}_9$, as described in Ref. 19. Such films are useful for extracting higher rank tensor properties of these materials, even in cases where bulk crystal growth is not possible, as in the case of $\text{Sr}_4\text{Bi}_4\text{Ti}_7\text{O}_{24}$.

In this letter, we report the determination of the thermal conductivity tensor of $\text{Sr}_4\text{Bi}_4\text{Ti}_7\text{O}_{24}$, an $n = 7$ member of the Aurivillius homologous series of phases, using epitaxial films with different orientations. Substrates of SrTiO_3 were used for deposition, with surface orientations of (100), (110), and (111). The phase purity of the films was confirmed by x-ray diffraction (XRD) and transmission electron microscopy (TEM). Thermal conductivity was characterized using time-domain thermoreflectance (TDTR).

Polycrystalline PLD targets with a Sr:Bi:Ti ratio of 4:4.6:7 were synthesized by mixing high-purity powders of Bi_2O_3 , TiO_2 , and SrCO_3 of at least 99.99% purity and sintering in air. The molar ratio corresponds to 15% excess bismuth over the resulting film composition ($\text{Sr}_4\text{Bi}_4\text{Ti}_7\text{O}_{24}$), estimated to be sufficient to compensate for bismuth volatility. Films were synthesized by PLD from this single target using 10,000 pulses of a KrF excimer laser, $\lambda = 248 \text{ nm}$, under $p_{\text{O}_2+\text{O}_3} = 90 \text{ mTorr}$, and at 767, 805, and 808 °C, respectively, for the SrTiO_3 single crystal substrates of three differing orientations—(100), (110), and (111). Temperature

^{a)}Author to whom correspondence should be addressed. Electronic mail: mark_z@mac.com.

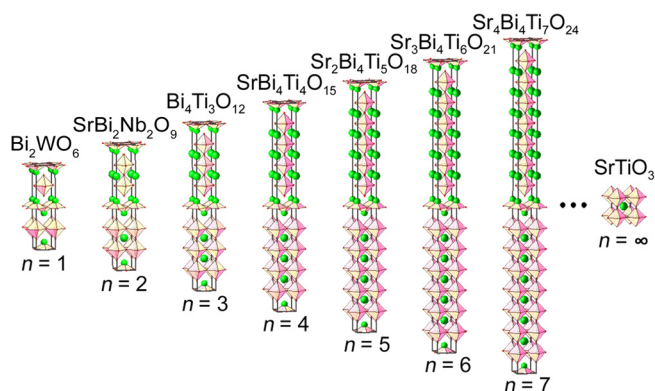


FIG. 1. The Aurivillius homologous series of phases, $\text{Bi}_2\text{A}_{n-1}\text{B}_n\text{O}_{3n+3}$. The structure consists of perovskite slabs separated by $\text{Bi}_2\text{O}_2^{2+}$ pyramidal layers. Small green spheres are Bi^{3+} , large green spheres are Sr^{2+} , and pink coordination octahedra are TiO_6^{2-} .

was maintained with a precision of $\pm 0.1^\circ\text{C}$ (precision of readout as measured by a type N thermocouple in the furnace cavity) using a pseudo-blackbody cavity furnace to contain and heat the substrate. The furnace consists of a platinum heating element cylindrically wound around an alumina tube, with a baffle at the open end to minimize heat loss. The substrate is held in the center of the heating zone on the end of a ceramic thermocouple tube so that the temperature is measured at the substrate. The furnace design is described in more detail in Ref. 22. Films were quenched immediately (< 3 s) after growth by dropping them onto the flat stainless

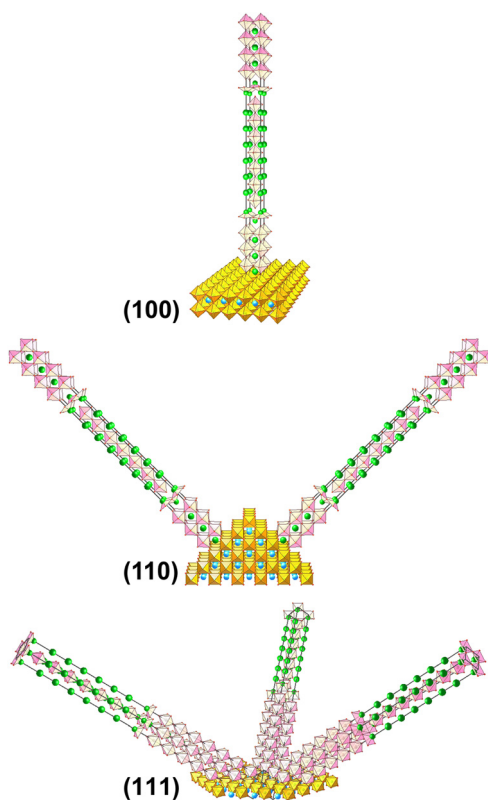


FIG. 2. Schematic showing the orientation relationship between the SrTiO_3 substrate surface and the resultant number of rotational twins for the three orientations used in this study, (100), (110), and (111). Colors are the same as in Fig. 1, with substrate shown in orange and cyan for clarity.

steel bottom of the vacuum chamber to avoid decomposition by volatilization of bismuth suboxides.²³

XRD characterization was performed using a four-circle diffractometer and $\text{Cu-K}\alpha$ radiation with a graphite incident-beam monochromator. Deposition conditions were tuned to maximize the extent of superlattice reflections and to minimize mosaic texture in the epitaxial films. Samples judged of highest quality were then selected for subsequent analysis. Cross-sectional TEM samples were prepared by focused ion beam (FIB) methods using a FEI Nova 600, in which an approximately $30\text{-}\mu\text{m}$ -wide lamella was trenced, plucked, and polished with gallium ions at successively lower accelerating voltages of 30, 10, and 5 keV. This process yields an electron-transparent sample, fixed to a copper mount with platinum. Thermal transport measurements along the axis perpendicular to the plane of the films were performed by the well-established TDTR non-contact technique of thermal measurement, which has been thoroughly validated and extensively applied in our studies of thin films. Both the thermal conductivity^{24,25} and the thermal interface conductance²⁶ were measured at room temperature. To perform TDTR, a thin metal susceptor layer is deposited on the surface of the thin film and is pumped with a short pulse of a 9.8 MHz laser beam. This thin layer equilibrates quickly, and its change in temperature is measured by the temperature-dependent change in reflectance of the metal. Full details of the method and analysis are described in Ref. 27. For analysis, heat capacities per unit volume were assumed to be similar to bulk SrTiO_3 , $2.7\text{ J/cm}^2\text{ K}$, based on its similar atomic density of the unit cell.

The films of $\text{Sr}_4\text{Bi}_4\text{Ti}_7\text{O}_{24}$ were found to be phase pure and epitaxially oriented to the underlying (100) SrTiO_3 , (110) SrTiO_3 , and (111) SrTiO_3 substrates. In prior work, we found $\text{Sr}_4\text{Bi}_4\text{Ti}_7\text{O}_{24}$ to be ferroelectric with a paraelectric-to-ferroelectric transition temperature of approximately 324 K.¹³ θ - 2θ XRD scans are shown in Fig. 3. No peaks

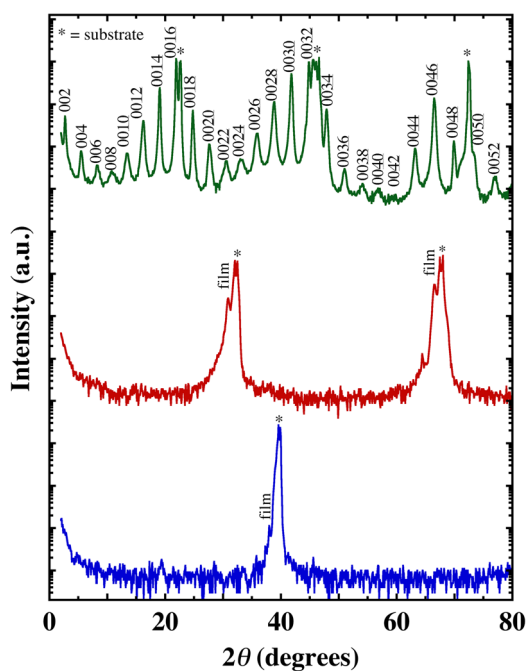


FIG. 3. XRD scans of the $\text{Sr}_4\text{Bi}_4\text{Ti}_7\text{O}_{24}$ films grown on (100), (110), and (111) SrTiO_3 substrates, respectively, from top to bottom.

from other orientations or phases are present. The full-width at half-maximum (FWHM) of the XRD rocking curve ω -scan of the 0032- peak of the film on (100) SrTiO₃ (not shown) is 0.50°. Epitaxy of the (001) oriented Sr₄Bi₄Ti₇O₂₄ sample on (100) SrTiO₃ was confirmed by a ϕ -scan of the 1013 peak of the Sr₄Bi₄Ti₇O₂₄ (not shown), with a FWHM of 2.1°. Analogous to the growth of other Aurivillius phases on (100), (110), and (111) perovskite substrates,^{17–21} the orientation relationship of Sr₄Bi₄Ti₇O₂₄ to the underlying perovskite substrate can be expressed in all three cases as Sr₄Bi₄Ti₇O₂₄ (001)||SrTiO₃ {100} and Sr₄Bi₄Ti₇O₂₄ [100]||SrTiO₃(010). The *c*-axes of the epitaxial Sr₄Bi₄Ti₇O₂₄ films remain aligned to the $\langle 100 \rangle$ axes of the SrTiO₃ for the three different substrate orientations. This causes the *c*-axis of Sr₄Bi₄Ti₇O₂₄ (the superlattice layering axis) to tilt by 0°, 45°, and 54.7° from the normal to the substrate for growth on (100), (110), and (111) SrTiO₃ substrates, respectively. The *c*-axis lattice parameter, calculated by a Nelson-Reilly regression fit of θ -2 θ peak positions of the sample on (100) SrTiO₃, is 64.7 ± 0.39 Å. The in-plane lattice parameter of its tetragonal unit cell, as determined from *c* and the ϕ -scan diffractometer angles, is $a = 3.88 \pm 0.025$ Å. We use tetragonal indexing throughout this paper.

TEM characterization is necessary for confirmation of large-period superlattice phases such as this, which are difficult to discern from intergrowths of multiple shorter-period members by XRD alone, due to the insensitivity of XRD to local disorder. Thus, TEM imaging and electron diffraction analysis must also be performed.^{14,28–30} For the (110) and (111) films, two orthogonal-viewing-axis samples of each were prepared and analyzed. TEM results are shown in Figs. 4(a) and 4(b), respectively. The cross-section TEM lattice images and diffraction patterns were taken from the same samples shown in Fig. 3, to provide confirmation of synthesis of the $n = 7$ Aurivillius phase for all of the orientations. The films are free of intergrowths of other- n Aurivillius phases. These are the longest-period Aurivillius phases ever synthesized in inclined epitaxial orientations. Epitaxy was also confirmed for all three orientations. In the sample grown on (111) SrTiO₃, ledge growth led to the inclusion of a significant amount of nanoporosity along in-plane $\langle 110 \rangle$ axes due to the highly anisotropic growth rates along the different crystalline axes, and to the angle of intersection of the rotation twin boundaries, which is aperiodic with the crystal structure of the film. Growth-twin boundaries and roughness were also observed in this sample, so its thermal conductivity results were excluded from tensor analysis.

TDTR analysis was performed on the *same volume of the same films* later used for the TEM characterization, within ~1 mm laterally, so that accurate thickness measurements could be made. The anisotropy of thermal transport in films of the Sr₄Bi₄Ti₇O₂₄ was made by TDTR measurements of the thermal transport behavior of the three films on grown on (100), (110), and (111) SrTiO₃. In these films, the superlattice layering is oriented at 0°, 45°, and 54.7° relative to surface-normal, respectively. The in-plane and out-of-plane components of thermal conductivity can be extracted from these values as described below. Fringing effects are considered minimal as the radius of the TDTR spot-size is 14 μ m, and films are on the order of 200 nm in thickness. We assume that

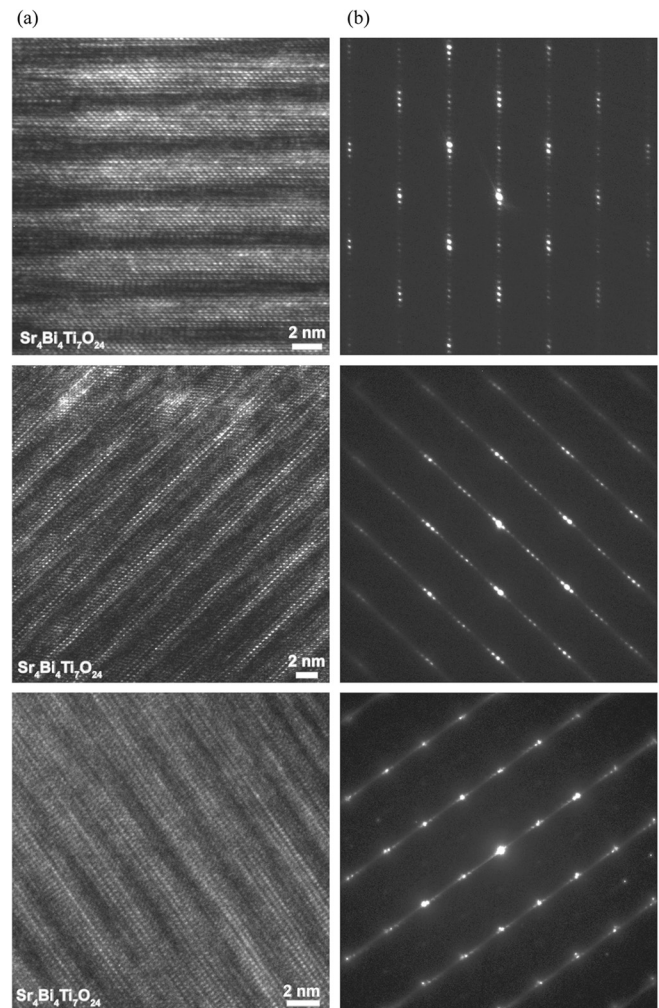


FIG. 4. Cross-sectional (a) high-resolution TEM (HRTEM) images and (b) electron nano-diffraction patterns of the three films grown on (100), (110), and (111) SrTiO₃ substrates, respectively, from top to bottom. The TEM images and diffraction patterns are oriented with respect to the plane of the substrate lying horizontally. One of two rotational twin (growth-twin) orientations is shown for the (110) film, and one of three rotational twin orientations for the (111) film. Superlattice reflections and HRTEM measurements confirm phase-pure and epitaxial synthesis of the $n = 7$ Aurivillius phase Sr₄Bi₄Ti₇O₂₄.

the effect of twin boundaries on the measured thermal conductivity is negligible, because the ratio of the in-plane spacing of the twin boundaries to the *c*-axis length of Sr₄Bi₄Ti₇O₂₄ is much larger than the extracted anisotropy of the thermal conductivity tensor, k_{33}/k_{11} .

The Sr₄Bi₄Ti₇O₂₄ films grown on both (100) and (110) SrTiO₃ are smooth and pore-free. Thus, the anisotropy of the thermal conductivity can be extracted from these samples using Eq. (1), based on the ellipsoidal shape of the longitudinal thermal conductivity (a second rank polar tensor) in Sr₄Bi₄Ti₇O₂₄,³¹

$$k_{\theta} = \sin^2 \theta k_{11} + \cos^2 \theta k_{33}, \quad (1)$$

where k_{θ} is the thermal conductivity measured at the angle θ to the [001] axis of Sr₄Bi₄Ti₇O₂₄ ($\theta = 0^\circ$ and 45° , respectively, for the Sr₄Bi₄Ti₇O₂₄ samples grown on (100) and (110) SrTiO₃), k_{11} is the thermal conductivity in the (001) plane of Sr₄Bi₄Ti₇O₂₄, and k_{33} is the thermal conductivity

perpendicular to the (001) plane of $\text{Sr}_4\text{Bi}_4\text{Ti}_7\text{O}_{24}$ (across the planes of the superlattice layering). In our measurements, $k_{0^\circ} = 1.10 \text{ W m}^{-1} \text{ K}^{-1}$ and $k_{45^\circ} = 1.45 \text{ W m}^{-1} \text{ K}^{-1}$. Therefore, $k_{33} = k_{0^\circ} = 1.10 \text{ W m}^{-1} \text{ K}^{-1}$ and $k_{11}, k_{22} = 1.80 \text{ W m}^{-1} \text{ K}^{-1}$. The k_{33}/k_{11} ratio is in approximate agreement with other results on the similar compound $\text{Bi}_4\text{Ti}_3\text{O}_{12}$ in Refs. 4 and 5.

In conclusion, we have determined the tensor of thermal conductivity of the $n = 7$ member of the Aurivillius homologous series, $\text{Sr}_4\text{Bi}_4\text{Ti}_7\text{O}_{24}$ by synthesis on single-crystal SrTiO_3 substrates with the superlattice layering oriented at 0° (100), 45° (110), and 54.7° (111) from the plane of the substrates used. XRD and TEM characterization showed the layers to be phase-pure and epitaxial. TDTR was used to measure the films' cross-plane thermal conductivities, enabling extraction of the superlattice's cross-plane and in-plane thermal conductivities.

This work was supported by the Defense Advanced Research Projects Agency (DARPA) and the U.S. Army Aviation and Missile Research, Development, and Engineering Center (AMRDEC).³² D.G.C. acknowledges support of the Air Force Office of Scientific Research MURI FA9550-08-1-0407. Sample preparation was performed by the UCLA Nanoelectronics Research Facility, and microscopy at the UCLA California Nanosystems Institute's (CNSI's) Electron Imaging Center for Nanomachines (EICN).

¹D. G. Cahill, W. K. Ford, K. E. Goodson, G. D. Mahan, A. Majumdar, H. J. Maris, R. Merlin, and S. R. Phillpot, *J. Appl. Phys.* **93**, 793 (2003).

²D. G. Cahill, A. Melville, D. G. Schlom, and M. A. Zurbuchen, *Appl. Phys. Lett.* **96**, 121903 (2010).

³D. G. Cahill, S. K. Watson, and R. O. Pohl, *Phys. Rev. B* **46**, 6131 (1992).

⁴B. Steele, A. D. Burns, A. Chernatynskiy, R. W. Grimes, and S. R. Phillpot, *J. Mater. Sci.* **45**, 168 (2010).

⁵Y. Shen, D. R. Clarke, and P. A. Fuierer, *Appl. Phys. Lett.* **93**, 102907 (2008).

⁶A. Chernatynskiy, R. W. Grimes, M. A. Zurbuchen, D. R. Clarke, and S. R. Phillpot, *Appl. Phys. Lett.* **95**, 161906 (2009).

⁷Y. Iwazaki, T. Suzuki, S. Sekiguchi, and M. Fujimoto, *Jpn. J. Appl. Phys., Part 2* **38**, L1443 (1999).

⁸J. H. Haeni, C. D. Theis, D. G. Schlom, W. Tian, X. Q. Pan, H. Chang, I. Takeuchi, and X. D. Xiang, *Appl. Phys. Lett.* **78**, 3292 (2001).

⁹K. Shibuya, S. Mi, C.-L. Jia, P. Meuffels, and R. Dittmann, *Appl. Phys. Lett.* **92**, 241918 (2008).

¹⁰M. Okude, A. Ohtomo, T. Kita, and M. Kawasaki, *Appl. Phys. Express* **1**, 081201 (2008).

¹¹W. Tian, J. H. Haeni, D. G. Schlom, E. Hutchinson, B. L. Sheu, M. M. Rosario, P. Schiffer, Y. Liu, M. A. Zurbuchen, and X. Q. Pan, *Appl. Phys. Lett.* **90**, 022507 (2007).

¹²M. A. Zurbuchen, R. S. Freitas, M. J. Wilson, P. Schiffer, M. Roeckerath, J. Schubert, G. H. Mehta, D. J. Comstock, J. H. Lee, Y. Jia, and D. G. Schlom, *Appl. Phys. Lett.* **91**, 033113 (2007).

¹³M. A. Zurbuchen, V. O. Sherman, A. K. Tagantsev, J. Schubert, M. E. Hawley, D. D. Fong, S. K. Streiffer, Y. Jia, W. Tian, and D. G. Schlom, *J. Appl. Phys.* **107**, 024106 (2009).

¹⁴M. A. Zurbuchen, J. Lettieri, G. Asayama, Y. Jia, S. Knapp, A. H. Carim, D. G. Schlom, X. Q. Pan, and S. K. Streiffer, *J. Mater. Res.* **22**, 1439 (2007).

¹⁵J. S. Anderson, *The Chemistry of Extended Defects in Non-metallic Solids: Proceedings of the Institute for Advanced Study on the Chemistry of Extended Defects in Non-metallic Solids*, edited by L. Eyring and M. O'Keefe (North-Holland, Amsterdam, The Netherlands, 1970), pp. 1–20.

¹⁶B. Aurivillius, *Ark. Kemi* **1**, 463 (1950); **1**, 499 (1950); **2**, 519 (1951); **5**, 39 (1953).

¹⁷J. Lettieri, M. A. Zurbuchen, Y. Jia, D. G. Schlom, S. K. Streiffer, and M. E. Hawley, *Appl. Phys. Lett.* **76**, 2937 (2000).

¹⁸J. Lettieri, M. A. Zurbuchen, Y. Jia, D. G. Schlom, S. K. Streiffer, and M. E. Hawley, *Appl. Phys. Lett.* **77**, 3090 (2000).

¹⁹D. G. Schlom, L.-Q. Chen, X. Q. Pan, A. Schmehl, and M. A. Zurbuchen, *J. Am. Ceram. Soc.* **91**, 2429 (2008).

²⁰H. Matsuda, M. Kurachi, H. Uchida, T. Watanabe, T. Iijima, S. Koda, and H. Funakubo, *Jpn. J. Appl. Phys., Part 2* **44**, L292 (2005).

²¹T. Watanabe and H. Funakubo, *J. Appl. Phys.* **100**, 051602 (2006).

²²J. C. Clark, J.-P. Maria, K. J. Hubbard, and D. G. Schlom, *Rev. Sci. Instrum.* **68**, 2538 (1997).

²³M. A. Zurbuchen, J. Lettieri, S. J. Fulk, Y. Jia, A. H. Carim, D. G. Schlom, and S. K. Streiffer, *Appl. Phys. Lett.* **82**, 4711 (2003).

²⁴C. Chiriac, D. G. Cahill, N. Nguyen, D. Johnson, A. Bodapati, P. Keblinski, and P. Zschack, *Science* **315**, 351 (2007).

²⁵Y. K. Koh, S. L. Singer, W. Kim, J. M. O. Zide, H. Lu, D. G. Cahill, A. Majumdar, and A. C. Gossard, *J. Appl. Phys.* **105**, 054303 (2009).

²⁶H.-K. Lyee and D. G. Cahill, *Phys. Rev. B* **73**, 144301 (2006).

²⁷D. G. Cahill, *Rev. Sci. Instrum.* **75**, 5119 (2004).

²⁸J. L. Hutchison, J. S. Anderson, and C. N. R. Rao, *Proc. R. Soc. London, Ser. A* **355**, 301 (1977).

²⁹J. Drennan, C. P. Tavares, and B. C. H. Steele, *Mater. Res. Bull.* **17**, 621 (1982).

³⁰J. M. Tarascon, W. R. McKinnon, P. Barboux, D. M. Hwang, B. G. Bagley, L. H. Greene, G. W. Hull, Y. LePage, N. Stoffel, and M. Giroud, *Phys. Rev. B* **38**, 8885 (1988).

³¹R. E. Newnham, *Properties of Materials: Anisotropy, Symmetry, Structure* (Oxford University Press, New York, 2005).

³²The views, conclusions contained in this document are those of the authors and should not be interpreted as representing the official policies, either expressed or implied, of the Defense Advanced Research Projects Agency; the U.S. Army Aviation and Missile Research, Development, and Engineering Center; or the U.S. Government.